Therapeutic Efficacy of ABT-737, a Selective Inhibitor of BCL-2, in Small Cell Lung Cancer

Christine L. Hann, Vincent C. Daniel, Elizabeth A. Sugar, Irina Dobromilskaya, Sara C. Murphy,
Leslie Cope, Xue Lin, Jared S. Hierman, Daniel L. Wilburn, D. Neil Watkins,
and Charles M. Rudin

Sidney Kimmel Comprehensive Cancer Center, Johns Hopkins University, Baltimore, Maryland

Abstract

Bcl-2 is a central regulator of cell survival that is overexpressed in the majority of small cell lung cancers (SCLC) and contributes to both malignant transformation and therapeutic resistance. We compared primary SCLC xenografts prepared from *de novo* human tumors with standard cell line–based xenografts in the evaluation of a novel and highly potent small molecule inhibitor of Bcl-2, ABT-737. ABT-737 induced dramatic regressions in tumors derived from some SCLC cell lines. In contrast, only one of three primary xenograft SCLC tumors showed significant growth inhibition with ABT-737. Explanations for this apparent dichotomy may include relatively low expression of Bcl-2 in the primary xenografts or inherent differences in the model systems. The addition of etoposide to ABT-737 in the primary xenografts resulted in significant decreases in tumor growth, underscoring the clinical potential of ABT-737 in combination therapy. To identify factors that may contribute to resistance to ABT-737 and related inhibitors, we isolated resistant derivatives of an initially sensitive cell line–based xenograft. Acquired resistance in this model was associated with decreases in the expression of the primary target Bcl-2, of proapoptotic partners of Bcl-2 (Bax and Bim), and of Bcl-2:Bim heterodimers. Expression profiling reveals 85 candidate genes demonstrating consistent changes in gene expression with acquired resistance. Taken together, these data have specific implications for the clinical development of Bcl-2 inhibitors for SCLC and broader implications for the testing of novel anticancer strategies in relevant preclinical models. [Cancer Res 2008;68(7):2321–8]

Introduction

Lung cancer is the leading cause of cancer deaths for both men and women in the United States (1). Small cell lung cancer (SCLC) accounts for ∼15% of all lung cancer cases and is distinguished from non-SCLC by its characteristic cellular appearance, rapid proliferation, and early dissemination to metastatic sites. Platinum-based chemotherapy induces responses in up to 70% of newly diagnosed SCLC and is the standard of care for this disease (2–4). However, responses to first line chemotherapy are typically of short duration, and the median survival from the time of diagnosis in patients with extensive stage SCLC remains <1 year. New approaches are needed in the management of SCLC.

Bcl-2 was the first identified member of a family of apoptotic regulators which have at least one Bcl-2 homology domain in common (5). Bcl-2 family members include antiapoptotic (prosurvival) proteins (e.g., Bcl-2, Bcl-x_L, and Mcl-1), multidomain proapoptotic proteins (e.g., Bax and Bak), and BH3-only proapoptotic proteins (e.g., Bim, Bid, Noxa, and Puma; ref. 5). Interactions between and relative ratios of proapoptotic and antiapoptotic Bcl-2 family members are key determinants of cellular sensitivity to multiple cell death triggers, including many standard chemotherapeutic agents.

Increased expression of Bcl-2 has been reported in 73% to 90% of SCLC cases and is associated with chemotherapeutic resistance in SCLC cell lines (6–8). Overexpression of Bcl-2 can abrogate chemotherapy-induced apoptosis in lung cancer cell lines (9). Conversely, inhibition of Bcl-2 by an antisense oligonucleotide results in cytotoxicity and regression of SCLC tumors in preclinical models. Initial clinical trials combining standard chemotherapy with an antisense oligonucleotide directed against bcl-2 mRNA (G3139; oblimersen) in patients with SCLC, however, did not show significant suppression of Bcl-2 protein levels *in vivo* (10). Consistent with inadequate target suppression, the addition of G3139 to standard chemotherapeutics did not result in improvements in objective response or clinical outcome (11).

Investigators at Abbott Laboratories used a combination of nuclear magnetic resonance structure-based design, high-throughput screening, and iterative lead compound optimization to identify a family of high-affinity, high-potency small molecule inhibitors of Bcl-2 and Bcl-x_L (12). ABT-737, a Bcl-2/Bcl-x_L inhibitor with affinity in the nanomolar range, has shown activity against several hematopoietic and solid tumor cell lines and xenografts (12–15). Based on these observations, an orally bioavailable derivative of ABT-737 is under early-phase clinical testing in patients with both solid tumors and hematologic malignancies.

Most preclinical therapeutic assessment in solid tumors (including all prior evaluation of ABT-737 efficacy) depends on cancer cell lines established *in vitro* and analyzed *in vivo* as cell line xenografts. Preclinical activity in cell line–based xenografts have not consistently predicted clinical efficacy of drugs (16). This failure of traditional models may be in part dependent on selective pressures that favor establishment and maintenance of cell lines as monolayers, in high glucose media and with the high oxygen tension typically present in tissue culture. None of these features is required for growth and spread of cancers *in vivo*. Molecular characterization of glioblastoma multiforme has shown that growth of primary glioblastoma multiforme tumor samples in standard serum-containing media (DMEM + 10% FCS), as used

for many commercially available cell lines, induced significant changes in gene expression and chromosomal alterations when compared with the original patient samples (17). An alternate model based on the direct transfer and propagation of human tumors cells in immunocompromised mice, primary xenografts, or heterotransplants promotes maintenance of tumor histologic features, biological behaviors, and gene expression profiles that closely resemble those of the parental tumor (18). These observations suggest that primary xenograft tumor models may represent a better platform for preclinical therapeutic testing, one that may be more predictive of ultimate clinical efficacy.

The aims of this study were to evaluate the activity of ABT-737 in two distinct models of SCLC, traditionally cultured SCLC cell lines with varying expression of Bcl-2, and primary SCLC xenografts derived from chemotherapy-naive patients, alone and in combination with cytotoxic chemotherapy. Based on observations of tumor recurrence and resistance in several of our xenografts, we have also initiated studies to look at mechanisms of ABT-737 resistance. Data on the efficacy of ABT-737 in SCLC cell lines and primary SCLC xenografts and mechanisms contributing to resistance to ABT-737 have direct implications for the clinical evaluation of Bcl-2 inhibitors in patients with SCLC.

Materials and Methods

Cell culture and reagents. The human SCLC cell lines NCI-H82, NCI-H146, NCI-H187, NCI-H209, and NCI-H345 were purchased from and grown in media recommended by American Type Culture Collection (ATCC). The H187-63AR derivative was isolated from a recurrent tumor as described in this report and was grown in media conditions used for H187 cells. ABT-737, obtained from Abbott Laboratories, was dissolved in DMSO for *in vitro* experiments. To prepare ABT-737 for injection, the drug was first mixed with propylene glycol, Tween-80, and D_5W (pH 1.0), then sonicated, and pH adjusted at 4 to 5. For all *in vivo* experiments, mice received i.p. injections (200 μL) of ABT-737 at 100 mg/kg/d for 21 consecutive days. Etoposide (Novaplus) was diluted in $1\times$ PBS.

Cell viability assays. Cells were collected by centrifugation after treatment with ABT-737 or DMSO. Cell pellets were resuspended in buffer containing $1\times$ PBS, 1% fetal bovine serum (FBS), 0.1% sodium azide and 2 μg/mL propidium iodide. Cells were run on a FACSCalibur flow cytometer and analyzed using CellQuest Pro software (Becton Dickinson). To calculate EC_{50} values, nonlinear regression with sigmoidal dose-response curves (variable slope) was performed using GraphPad Prism version 4.00 for Windows (GraphPad Software). Assays were performed in triplicate.

Western blot. Whole-cell lysates were prepared in radioimmunoprecipitation assay buffer supplemented with protease and phosphatase inhibitors. Protein concentrations were determined by Bradford protein assay (Bio-Rad Laboratories). Equal protein concentrations of each sample were run on NuPAGE *bis*-Tris gels (Invitrogen) and electrophoretically transferred to polyvinylidene difluoride membranes. Membranes were blocked with TBS containing 5% skim milk and 0.1% Tween 20 and then probed with antibodies against Bcl-2, Bcl-x_L, Noxa, Bax, Bid, and Actin (all at 1:1,000; Santa Cruz Biotechnology), Mcl-1 (1:1,000; BD PharMingen), and Bim (1:1,000; Calbiochem). Blots were developed using enhanced chemiluminescence kit (Amersham Biosciences) according to the manufacturer's instructions.

Immunoprecipitations. Whole-cell lysates were prepared in Triton X-100 buffer (50 mmol/L Tris-HCl, 150 mmol/L NaCl, 5 mmol/L MgCl₂, 1 mmol/L EGTA, 10% glycerol, 1% Triton X-100). Total protein (400 μg) was precleared with 12 μL (of a 50% slurry) of protein A/G beads (Santa Cruz Biotechnology). The cleared lysates were incubated overnight at 4°C with protein A/G beads preexposed for 1 h to anti–Bcl-2 antibody (6C8, PharMingen). Immunoprecipitates were then washed thrice with Triton X-100 buffer and boiled in loading buffer (Invitrogen). Immunoblotting was performed as described above.

Caspase-3/caspase-7 assay. SCLC cell lines were treated with ABT-737 at the indicated doses and assayed for caspase-3/caspase-7 activity. Equilibrated caspase-Glo 3/7 reagent (Promega) was added to each well after 24 h of treatment. Luminescence was measured using a Perkin-Elmer Vision 3. Blank values were subtracted, and fold-increase in activity over untreated cells was calculated. Assays were performed in triplicate.

SCLC cell line xenografts. Adult homozygous nude mice (Charles River Laboratories) were s.c. injected with 5 to 8×10^6 cells suspended in PBS and Matrigel (BD Biosciences). The nude mice were either injected bilaterally (H82, H146, H187, H209, and H345) or unilaterally (H187-63AR). Once the tumors reached ≥ 150 mm^3, calculated as $V = L \times W^2 / 2$, mice were treated with i.p. injections of ABT-737 at 100 mg/kg/d or vehicle control. Serial measurements were taken with a manual caliper. Tumor responses were plotted with a nonlinear regression curve fit program (GraphPad Prism version 4.00 for Windows, GraphPad Software).

Primary SCLC xenografts. Primary xenografts LX22, LX33, and LX36 were derived from patients with treatment-naive extensive stage SCLC. In brief, tumor cells isolated from pleural effusion (LX22) or bronchoscopic biopsy (LX33, LX36) specimens were prepared into single-cell suspensions, mixed with Matrigel, and directly injected s.c. into NOD/SCID mice. All primary xenografts were maintained solely in immunocompromised mice by serial passaging. Primary xenografts were stained with H&E and CD56 at various passages to verify that they consistently maintained SCLC histology and cell surface staining characteristics.

For ABT-737 studies, freshly isolated primary xenograft tumors were mechanically dissociated into single-cell suspensions; 1×10^6 viable cells were resuspended in equal volumes of PBS and Matrigel and injected s.c. in adult homozygous C.B-17/SCID mice (Charles River Laboratories). Once the tumors reached ≥ 130 mm^3 (average, 14 d), the mice were treated with vehicle control, ABT-737 (100 mg/kg/d on days 1–21), etoposide (12 mg/kg/d on days 1, 4, and 9), or a combination of ABT-737 and etoposide.

Statistical analyses were performed for each primary xenograft separately. Initial tumor volume measurements are summarized using means, SDs, and ranges. Growth patterns were summarized graphically by plotting the mean and SD for each treatment group over time. The rate of growth is modeled using a log-linear random effects model. This model takes into account the correlation between multiple measurements on each mouse. The estimated growth rate per day is reported with 95% confidence intervals. A conditional *t* test is used to compare etoposide, ABT-737, and combination treatment with the control. A *P* value of <0.05 is considered statistically significant.

Immunohistochemistry. Formalin-fixed, paraffin-embedded tumors were sectioned, dewaxed, and incubated in 10 mmol/L sodium citrate (pH 8) for 20 min at 95°C for antigen retrieval. Sections were stained using the Vectastain ABC system according to manufacturer's instructions with a rabbit anti-CD56 antibody (Chemicon). To assess for apoptosis, LX22 tumors were collected after five consecutive days of ABT-737 treatment. The sections were prepared as described above and incubated with anti-activated caspase-3 antibody (Cell Signaling Technologies) and visualized using an horseradish peroxidase–conjugated secondary antibody and 3,3′-diaminobenzidine reagent (Dako Envision+, Dako).

Illumina microbead array. Total RNA was extracted using the Trizol reagent method (Invitrogen) and purified with RNAeasy columns (Qiagen). RNA quality was assessed using an Agilent 2100 Bioanalyzer (Agilent Technologies). RNA samples were labeled according to the chip manufacturer's recommended protocols. In brief, 0.5 μg of total RNA from each sample was labeled using the Illumina TotalPrep RNA amplification kit (Ambion) in a process of cDNA synthesis and *in vitro* transcription. Single-stranded RNA (cRNA) was generated and labeled by incorporating biotin-16-UTP (Roche Diagnostics GmbH) and hybridized to an Illumina Sentrix Human Ref-8 Expression Beadchip (Illumina). The hybridized biotinylated cRNA was detected with streptavidin-Cy3 and quantitated using an Illumina BeadStation 500GX genetic analysis systems scanner.

Illumina gene set analysis. Two biological samples from each tumor (H187 and H187-63AR) were hybridized to an Illumina BeadChip. Image level analysis and preprocessing was performed using BeadStudio software

(Bead Studio Gene Expression Module Users Guide May 2006) according to manufacturers recommendations. The preprocessing algorithm includes outlier detection and produces an average expression value for each oligonucleotide probe sequence. Data analysis and plotting of the expression profiles was done using the *R* statistical platform (19) and the Bioconductor bioinformatics software project (20). Preprocessed expression values were transformed to a log scale and averaged over replicates for each of the experimental conditions. Genes having log 2-fold changes >1 were used to cluster samples for comparison and presentation.

Real-time PCR. RNA was isolated from H187-63AR and H187 tumors by Trizol extraction. cDNA was prepared from using the Quantitect Reverse Transcription kit (Qiagen). Predesigned and validated gene-specific probe-based TaqMan gene expression assays for *CEPBD*, *FZD9*, *GPX2*, *NELL1*, *PRSS3*, *RTN1*, and *STMN2* (Applied Biosystems) were used for quantitative PCR. β-Actin gene (*ACTB*) was used as a control. The accumulation of amplicons during the reaction was detected by FAM Green (Applied Biosystems). The data were analyzed using the Bio-Rad iQ5 (version 2.0) software. Gene expression was analyzed from three parallel plates for each group. Each sample was run in triplicate for an individual plate.

Results

Effect of ABT-737 on cell viability and caspase-3 activation in SCLC cell lines. Western analysis of lysates from five SCLC cell lines showed that H146, H187, H209, and H345 cell lines expressed relatively high levels of the primary target of ABT-737, Bcl-2, whereas the H82 cell line expressed very low levels of Bcl-2 (Fig. 1*A*). All five cell lines expressed similar levels of Bcl-x_L. We then assessed the effect of ABT-737 treatment on these five SCLC cell lines. Cell lines were incubated in media containing 0.03 to 100 μmol/L ABT-737. The EC_{50} for each cell line was defined as the dose of ABT-737 required to cause 50% loss in viability of cells at 48 hours. Four of the five SCLC cell lines, H146, H187, H209, and H345, had EC_{50} values ranging from 0.06 to 0.5 μmol/L. The NCI-H82 cells were less sensitive to ABT-737, with an EC_{50} of 17.5 μmol/L (Fig. 1*B*).

To evaluate the target specificity of the responses seen in sensitive and less sensitive SCLC cell lines, the ability of ABT-737 to activate apoptosis in H146 and H82 cells was assessed by cleavage of a DEVD-containing luminescent substrate. ABT-737 induced significant caspase activation in H146 cells by 24 hours at a pharmacologic dose (0.06 μmol/L) consistent with target inhibition

in Bcl-2–dependent cells (Fig. 1*C*). In contrast, at 24 hours, ABT-737 was unable to induce significant capase-3 activation in H82 cells at 100 μmol/L, a dose of >5 × EC_{50}, suggesting that the toxicity of ABT-737 in H82 cells may be due to off-target effects.

Antitumor effect of ABT-737 on SCLC cell line xenografts. We next wanted to assess the *in vivo* activity of ABT-737 against xenografts derived from cell lines of differing *in vitro* sensitivities. Nude mice bearing xenografts derived from the H82, H146, H187, H209, and H345 SCLC lines were treated i.p. with ABT-737 or control vehicle for 21 days (Fig. 2). H146 and H187 xenografts rapidly regressed after the initiation of treatment with ABT-737. In particular, H187 xenograft tumors regressed below the level of detection by day 14, an effect which lasted for at least 7 days after the completion of treatment (H187 data shown in Fig. 3*A*). H209 and H345 xenografts showed intermediate sensitivity to ABT-737, with statistically significant decreases in growth rate and doubling time. Consistent with the *in vitro* data, H82 xenografts were resistant to the effects of ABT-737. Most H82 mice, regardless of treatment arm, were sacrificed before completion of the planned 21-day treatment due to rapidly increasing tumor size and ulceration.

A cell line derived from a recurrent ABT-737–resistant tumor maintains moderate resistance *in vitro* and *in vivo*. Acquired therapeutic resistance even after dramatic initial response is a major clinical problem in the management of SCLC. Treatment of H187 xenografts with ABT-737 resulted in evident complete antitumor responses. However, with continued monitoring of treated animals, we observed that some of the tumors recurred after the completion of therapy (Fig. 3*A*). To assess whether these tumors were still ABT-737 sensitive, we re-treated two mice with recurrent tumors with a second 21-day cycle of ABT-737 (arrow). Both recurrent tumors continued to progress despite treatment, consistent with acquired resistance to the drug. A cell line, H187-63AR, was derived from one of these recurrent tumors and maintained *in vitro* without ABT-737. *In vitro*, this derivative cell line had an EC_{50} of 0.5 μmol/L, ∼5× higher than that of the parental H187 cell line (data not shown).

To test whether H187-63AR cells maintained ABT-737 resistance *in vivo*, nude mice were injected s.c. to establish H187-63AR xenograft tumors. When the tumors reached ≥150 mm³, the mice
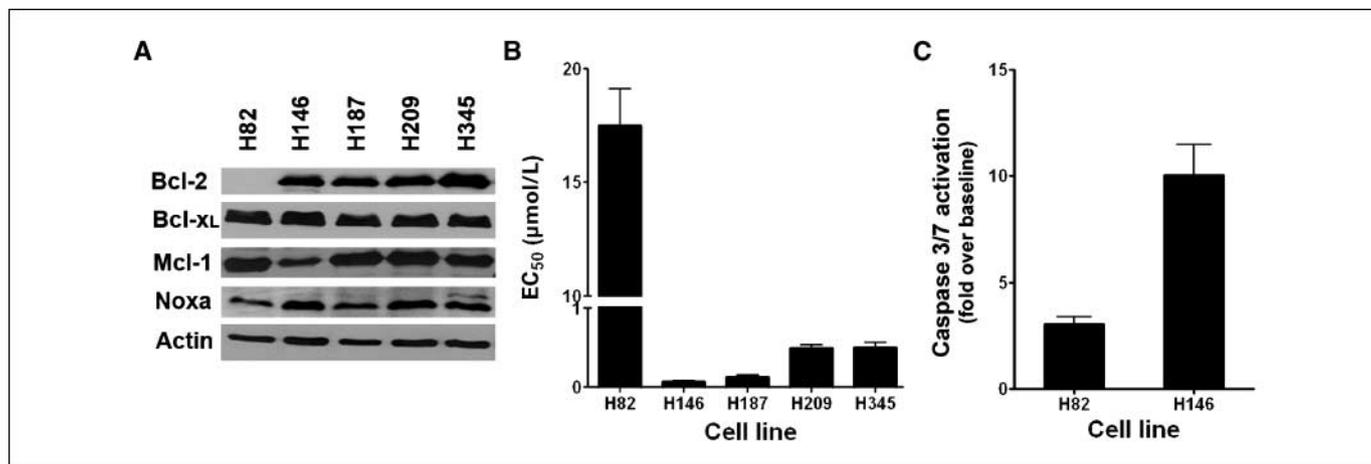

Figure 1. Cytotoxic activity of ABT-737 against a panel of SCLC cell lines correlates with Bcl-2 expression. *A,* lysates of the five SCLC cell lines were probed for Bcl-2, Bcl-x_L, Mcl-1, Noxa, and Actin. *B,* cell viability EC_{50} values of the same SCLC cell lines after treatment with ABT-737 was determined by propidium iodide exclusion and assayed by flow cytometry. *Columns,* average (*n* = 3) of triplicate experiments; *bars,* SD. *C,* caspase-3/caspase-7 activation after 24 h of treatment at the EC_{50} for H146 and at 5× the EC_{50} for H82. *Columns,* activation of caspase-3/caspase-7 over DMSO control.
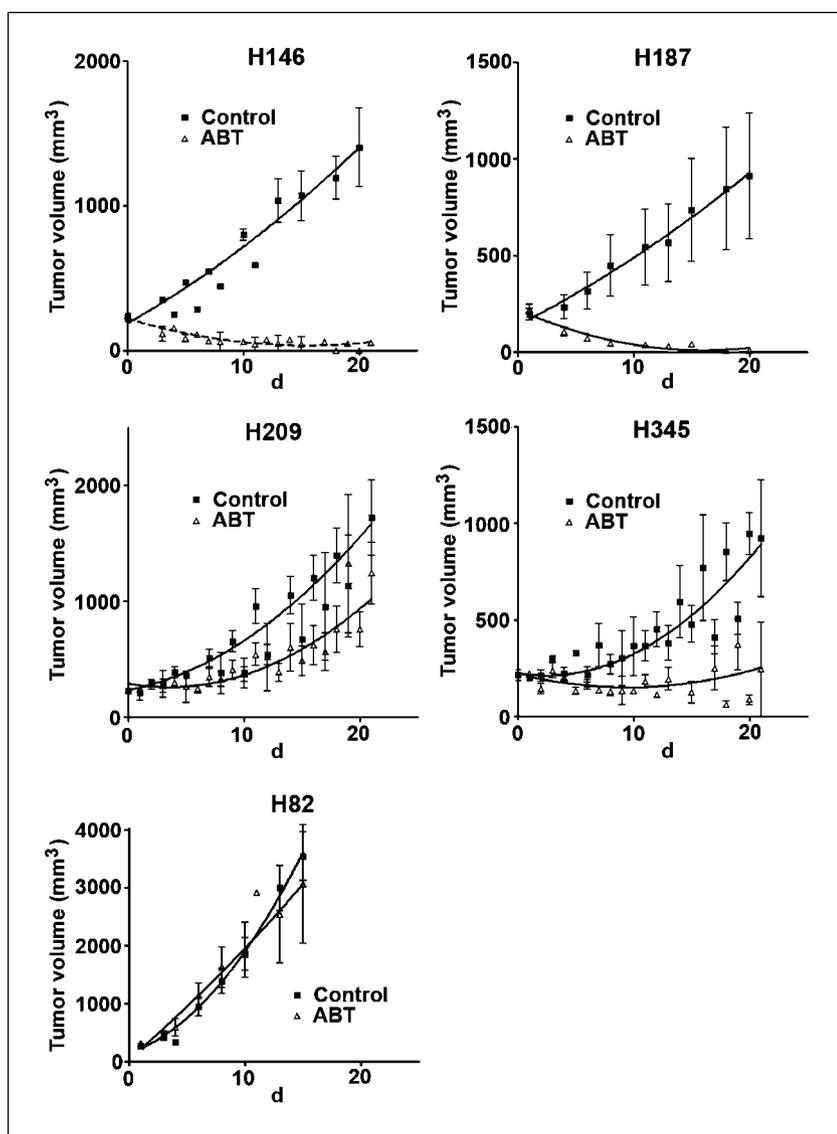
Figure 2. *In vivo* activity of ABT-737 against xenografts derived from SCLC cell lines. Tumor growth of SCLC xenografts on mice treated with vehicle control (*black squares*) or ABT-737 (*open triangles*) at 100 mg/kg/d i.p. for 21 d. Treatment was started on day 1. *X* axis, days after the initiation of treatment.

were randomized to receive vehicle or ABT-737 for 21 days. Nude mice bearing parental H187 xenografts were treated in parallel. H187-63AR control tumors grew at similar rates as H187 control tumors, suggesting that changes mediating ABT-737 resistance in this cell line did not alter basal tumor growth rates (Fig. 3*B*). As seen previously, H187 tumors completely regressed within 2 weeks of starting ABT-737 therapy. ABT-737–treated H187-63AR xenografts showed an intermediate phenotype, with a decrease in growth rate but no tumor regression, consistent with acquired resistance to the drug.

To identify putative determinants of acquired ABT-737 resistance, we first compared expression of Bcl-2 family members in parental and resistant H187 tumors. Western analysis of tumor lysates showed that the expression of Bcl-2, Bax, and particularly Bim were decreased in the H187-63AR tumors relative to H187 tumors (Fig. 3*C*). Abundance of Bcl-2:Bim complexes has recently been reported as a correlate of ABT-737 sensitivity in lymphoma cells. To test whether there was a change in Bim association with Bcl-2 in the resistant derivative, we performed immunoprecipitations on H187 and H187-63AR lysates using anti–Bcl-2 antibodies. Consistent with the results in lymphoma lines, we found that H187-

63AR cells had significantly less Bim complexed with Bcl-2 than did H187 cells (Fig. 3*C*).

As an initial probe for additional factors that may contribute to ABT-737 resistance, we compared the gene expression profiles of two independent H187-63AR–derived tumors with those of parental H187 tumors by Illumina microbead array analysis (GEO accession number GSE10003). A cutoff of at least a 2-fold change in expression was considered to be a minimal change of interest. This analysis defined a panel of 85 candidate genes that seem to be significantly differentially expressed in parental versus ABT-737–resistant derivatives of H187 (Fig. 3*D*; Supplementary Table S1). From the list, we selected seven genes (*CEBPD*, *FZD9*, *GPX2*, *NELL1*, *PRSS3*, *RTN1*, and *STMN2*) implicated in tumorigenesis and assessed their expression by quantitative PCR. Validating the microarray data, we found that *CEPBD*, *FZD9*, *NELL1*, and *PRSS3* expression was decreased and that *GPX2*, *RTN1*, and *STMN2* expression was increased in H187-63AR tumors compared with H187 tumors (Supplementary data). Confirmation of the roles of these candidate genes as factors contributing to ABT-737 resistance will require cross-validation in independent models of acquired resistance and individual gene expression cloning.

SCLC primary xenografts maintain characteristics of human SCLC. The primary SCLC xenografts used in this study were serially passaged in immunocompromised mice. H&E staining of the tumors shows the tumors maintain morphologic characteristics of SCLC (Fig. 4). Serially passaged tumors from all three primary SCLC xenografts maintain consistent expression of CD56 (neural cell adhesion molecule, an antigen expressed in the vast majority of SCLC; ref. 21) as assessed by immunohistochemistry (Fig. 4) and flow cytometry (data not shown).

ABT-737 induces apoptosis and exhibits synergistic effects with etoposide against primary SCLC xenografts. To assess the expression of Bcl-2 and Bcl-x_L in three SCLC primary xenografts, we performed Western analysis on lysates from freshly isolated tumors. Compared with the H345 SCLC cell line, LX22, LX33, and LX36 tumors express lower levels of Bcl-2, but comparable levels of Bcl-x_L and Mcl-1 (Fig. 5A). To evaluate whether ABT-737 was able to induce apoptosis in primary xenografts, LX22 tumors were harvested after five consecutive days of ABT-737 treatment and stained for activated caspase-3 by immunohistochemistry. Despite

the relatively low levels of Bcl-2 in the LX22 xenografts, treatment with ABT-737 resulted in activated caspase-3–positive cells *in vivo* (Fig. 5B).

We next wanted to assess whether the dramatic antitumor activity of ABT-737 seen in most standard cell line–based xenografts would be reflected in a similar activity in the primary xenograft model and further assess this activity compared with that of a standard clinically available cytotoxic agent. C.B-17/SCID mice bearing LX33 primary xenografts were treated with ABT-737, etoposide, or vehicle control. Treatment with either etoposide or ABT-737 caused similar decreases in tumor growth rate, but neither resulted in prolonged antitumor response (Fig. 6A; Supplementary Table S2). For studies in LX22 and LX36 primary xenografts, we added a fourth arm, combination treatment with etoposide and ABT-737. In LX22 primary xenografts, treatment with ABT-737 or etoposide monotherapy resulted in minor, but statistically significant decreases in tumor growth and combination treatment had a greater effect than either single agent (Fig. 6B). In LX36 primary xenografts, etoposide monotherapy caused a significant
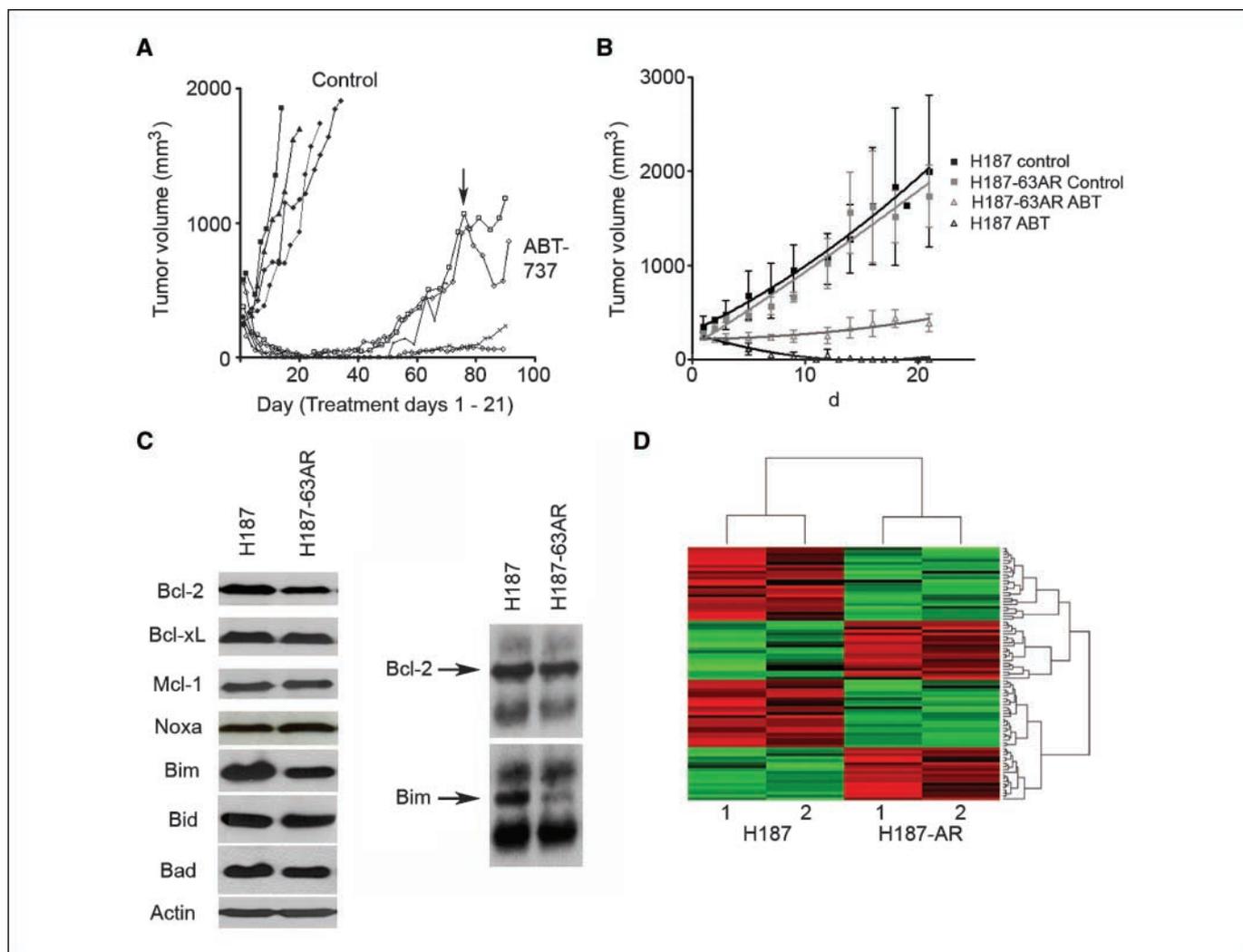

Figure 3. A SCLC cell line derived from an H187 ABT-737–resistant tumor maintains intermediate resistance *in vitro* and *in vivo*. *A,* H187 tumors recurred as early as 7 d after the completion of treatment. At day 76 (*arrow*), two mice were treated with a second cycle of ABT-737 at 100 mg/kg/d for 21 d. The H187-63AR cell line was derived from an ABT-resistant H187 tumor and grown in RPMI supplemented with 10% fetal bovine serum without ABT-737. *B,* mice bearing H187 parental tumors (*black*) and H187-63AR tumors (*gray*) were treated with vehicle control (*squares*) or ABT-737 (*open triangles*) at 100 mg/kg/d i.p. for 21 d; *X* axis, days after the initiation of treatment. *C, left,* lysates from H187 and H187-63AR cells were probed for Bcl-2, Bcl-x_L, Mcl-1, Noxa, Bim, Bid, Bad, and Actin; *right,* immunoblot of immunoprecipitates of H187 and H187-63AR lysates using an anti–Bcl-2 antibody. *D,* heat map of gene expression profiles of H187 and H187-63AR tumors.
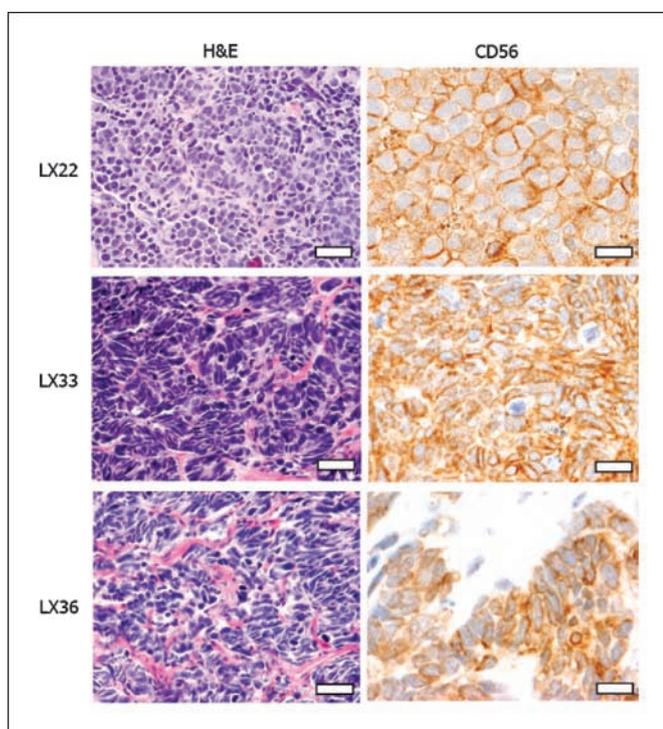
Figure 4. Initial characterization of primary xenografts: H&E and CD56 (neural cell adhesion molecule) staining of early passage tumors from each primary xenograft.

decrease in tumor growth, but ABT-737 alone did not. The combination of ABT-737 plus etoposide resulted in a statistically significant decrease in tumor growth rate compared with control (Fig. 6C). Taken together, these data show that the primary xenograft tumors were less responsive to ABT-737 than most xenografts derived from *ex vivo* SCLC cell lines.

Discussion

ABT-737 binds Bcl-2 and Bcl-x$_L$ with high affinity and has shown single-agent efficacy against multiple myeloma, acute myeloid leukemia, lymphoma, and solid tumor cell lines. It has also shown activity in combination with standard therapy in human leukemia and multiple myeloma models (22–24). We first evaluated ABT-737 efficacy in a panel of five SCLC cell lines and observed a range of sensitivity *in vitro* and *in vivo*. Consistent with the known mechanism of ABT-737, the H82 cell line which expresses very low levels of Bcl-2 was relatively resistant to ABT-737 *in vitro* and *in vivo*, and the cytotoxicity seen in this line at a high ABT-737 dose was nonapoptotic. Given that H82 cells express Bcl-x$_L$, which is also inhibited by ABT-737, the growth of H82 may be Bcl-2 and Bcl-x$_L$ independent. The remaining four cell lines expressed higher, closely matched levels of Bcl-2. Among these four cell lines, we found that *in vivo* antitumor efficacy correlated with *in vitro* EC$_{50}$ data; H146 and H187 cells had the lowest EC$_{50}$ values and completely regressed with ABT-737 treatment *in vivo*. H209 and H345 cells had higher, although still micromolar, EC$_{50}$ values than did the H146 and H187 cell lines and showed intermediate sensitivity to ABT-737 *in vivo*.

As an approach to identifying mechanisms of ABT-737 resistance in SCLC cell lines, we initiated studies to characterize recurrent, ABT-737–resistant tumors derived from H187 SCLC xenografts. A cell line established from one of these ABT-737–resistant tumors, H187-63AR, maintained relative resistance to ABT-737 *in vitro* and *in vivo*. Recent work in lymphoma cell lines showed that Bcl-2, Bim, and Bax levels and Bcl-2:Bim and Bcl-2:Bax interactions correlated with ABT-737 sensitivity. Of these associations, Bcl-2 expression and increased Bcl-2:Bim interactions, either of which might signify cellular dependence on Bcl-2, were the strongest predictors of ABT-737 sensitivity (25). We found that the H187-63AR cells express lower levels of Bcl-2, Bax, and Bim than H187 cells. Furthermore, we found that H187-63AR cells had lower abundance of Bim complexed with Bcl-2. Alterations in Bcl-2 family members, particularly decreased Bim and Bcl-2–associated Bim, may contribute to the ABT-737 resistance we observed in H187-63AR–derivative cells.

We also used cDNA microarray analysis to identify 85 genes whose expression was altered >2-fold between the parental and ABT-737–resistant tumors. To validate the microarray data, we confirmed differential expression of seven genes implicated in tumorigenesis by real-time PCR. Consistent with the microarray
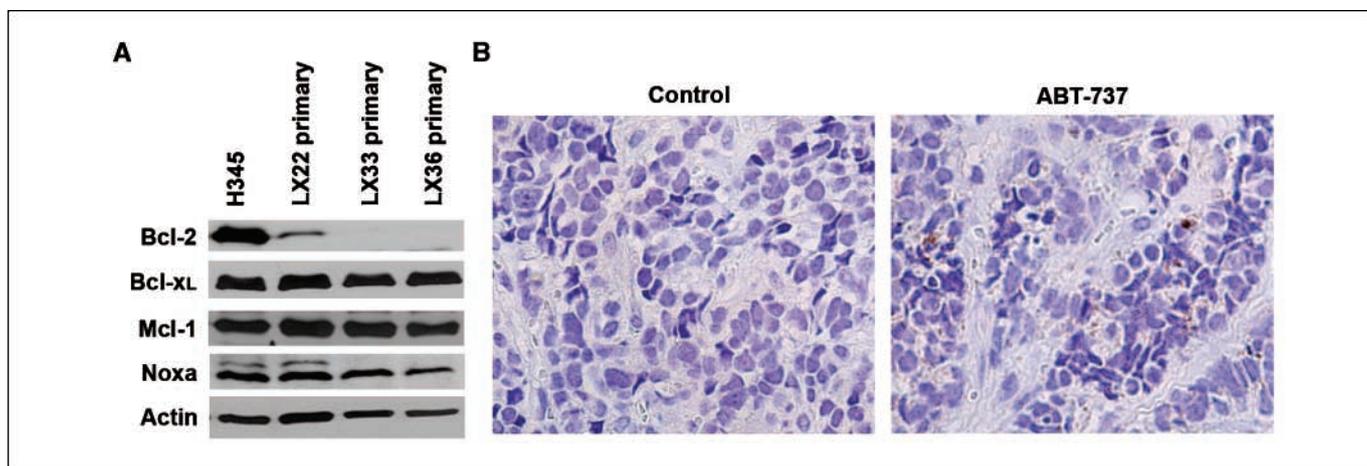

Figure 5. Activity of ABT-737 against SCLC primary xenografts. *A,* lysates from LX22, LX33, and LX36 primary xenografts probed with Bcl-2, Bcl-x$_L$, Mcl-1, Noxa, and Actin; lysates from the H345 SCLC cell line used as a reference. *B,* caspase-3 activation in an LX22 tumor after i.p. injection of ABT-737.
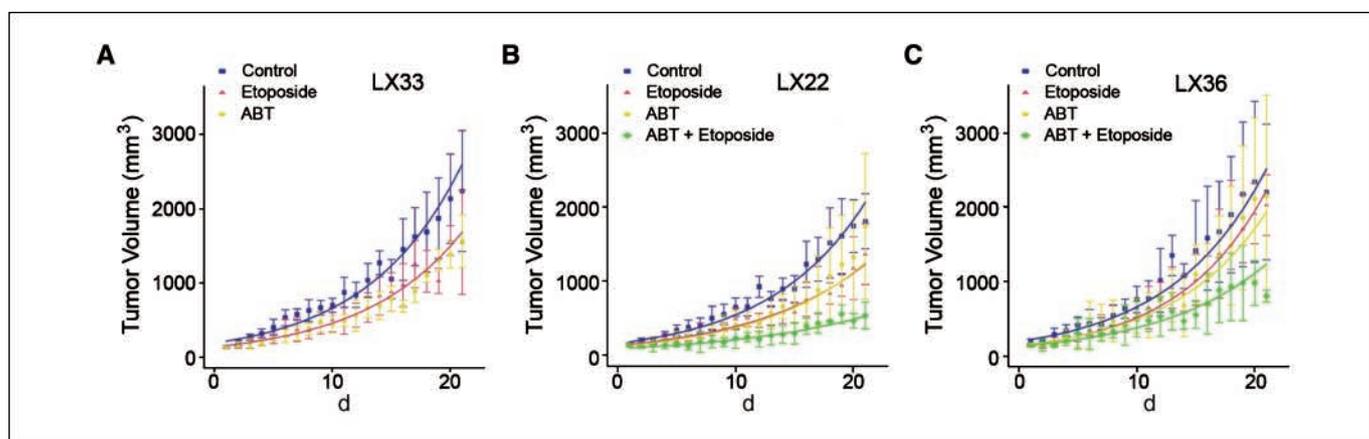
Figure 6. *In vivo* studies of ABT-737 or etoposide in LX33 primary xenografts (*A*) or ABT-737, etoposide or combination of ABT-737 and etoposide in LX22 (*B*) and LX36 (*C*) primary xenografts. Tumor growth of SCLC primary xenografts on mice treated with vehicle control (*blue*), ABT-737 (*yellow*) at 100 mg/kg/d i.p. for 21 d, etoposide (*red*) at 12 mg/kg/d for days 1, 4, and 9 or ABT-737 plus etoposide (*green*). X axis, days after the initiation of treatment.

data, we found up-regulation of *GPX2*, *RTN1*, and *STMN2* and down-regulation of *CEBPD*, *FXD9*, *NELL1*, and *PRSS3*. Further characterization of these genes may aid in the identification of factors that contribute to ABT-737 resistance and ultimately may help predict response to ABT-737.

We expanded our preclinical studies to include a model system not dependent on *ex vivo* selection of tumor cells for growth in tissue culture. Several studies support the utility of primary xenografts as a model system for prediction of clinical drug efficacy. To date, ABT-737 has been evaluated in primary models of hematologic malignancies, including multiple myeloma and leukemia. ABT-737 was able to induce apoptosis in primary multiple myeloma and primary acute myelogenous leukemia (AML) samples treated *ex vivo* (13, 14). ABT-737 enhanced the efficacy of dexamethasone, vincristine, and L-aspariginase in a primary *in vivo* model of acute lymphoblastic leukemia (24).

A primary xenograft model of SCLC has not been previously reported. We established three primary SCLC xenografts as a model system to evaluate ABT-737 and other novel SCLC therapeutics. All three primary xenografts were derived from therapy-naive SCLC patients and maintained the histologic appearance and CD56 antigen staining patterns of SCLC.

In contrast to its efficacy against most SCLC cell line–based tumors, ABT-737 did not cause regression of the primary SCLC xenografts. Treatment with ABT-737 monotherapy, however, reduced the growth rate of LX22 tumors, which had the highest expression of Bcl-2 among the three primary xenografts. ABT-737 did not show significant single-agent activity against the LX33 or LX36 primary xenografts. Our finding that cell line xenografts were more sensitive to ABT-737 monotherapy than were the primary xenografts could be due to several factors, including relative expression of and dependence on Bcl-2 or other Bcl-2 family members and inherent characteristics of patient tumors selected for growth in immunocompromised mice.

In contrast to published observations that Bcl-2 is expressed in the majority of SCLC cases and SCLC cell lines, all three primary xenografts in this study express low levels of Bcl-2. It is unlikely that direct transfer of tumors cells into immunocompromised mice selects for Bcl-2–independent tumors as Bcl-2 expression has been shown in primary xenografts derived from other tumor types (26–28). The three primary xenografts were derived from patients with treatment-naive SCLC. This stands in contrast to most avail-

able SCLC cell lines, which are derived from multiply pretreated disease. Evaluation of ABT-737 in additional primary SCLC xenograft models derived from *de novo* as well as recurrent tumors may help better define its potential role as monotherapy or in the second-line setting.

It is likely that ultimate clinical utility of agents, such as ABT-737, will require combination therapy with standard cytotoxic agents. In addition to evaluating single-agent activity in the primary xenograft model, we sought to test whether ABT-737 could enhance the activity of etoposide, a first-line agent in the treatment of SCLC and a potent inducer of apoptosis. In both primary xenografts tested, LX22 and LX36, the combination of ABT-737 and etoposide, caused statistically significant decreases in tumor growth rates relative to control. That ABT-737 can enhance to the activity of etoposide, even in low Bcl-2–expressing tumors, further supports its potential for clinical use.

Expression of antiapoptotic Bcl-2 family members not inhibited by ABT-737, in particular Mcl-1, has been implicated as a determinant of ABT-737 resistance. Reduction of Mcl-1 by small interfering RNA or targeted therapy can overcome ABT-737 resistance in multiple *in vitro* models (29, 30). In SCLC cell lines chronically exposed to ABT-737, ABT-737 resistance was associated with increased expression of Mcl-1 and decreased expression of proapoptotic Noxa (31). As all three primary xenografts express Mcl-1, other agents to consider in combination with ABT-737 could include Mcl-1–targeted therapies. Sorafenib, a Food and Drug Administration–approved agent in the treatment of renal cell carcinoma, has been shown to decrease Mcl-1 in an AML model (32). Cisplatin, a first-line agent in the treatment of SCLC, decreases Mcl-1 levels in human renal tubular epithelial cells (33). The primary xenografts may serve as representative models that test combinatorial therapies with agents that down-regulate multiple members of the Bcl-2 family.

As an oral derivative of ABT-737, ABT-263 has recently been introduced into phase I/phase II clinical trials; the identification of determinants of sensitivity to this agent has significant clinical implications. Preclinical studies of ABT-737 to date, including the studies presented here, show ABT-737 efficacy against tumors which express high levels of Bcl-2. Our work with primary SCLC xenografts revealed that, in combination with cytotoxic chemotherapy, such as etoposide, ABT-737 may have utility even in tumors which express low levels of Bcl-2. Combinatorial therapy designed to inhibit multiple members of the Bcl-2 family may be an interesting avenue

for future studies. Further evaluation of drug resistant derivative tumors may provide information on factors and pathways that will guide clinical development of the targeted Bcl-2 inhibitors.

Acknowledgments

References

1. Jemal A, Siegel R, Ward E, Murray T, Xu J, Thun MJ. Cancer statistics, 2007. CA Cancer J Clin 2007;57:43–66.
2. Slevin ML, Clark PI, Joel SP, et al. A randomized trial to evaluate the effect of schedule on the activity of etoposide in small-cell lung cancer. J Clin Oncol 1989;7:1333–40.
3. Johnson BE, Crawford J, Downey RJ, et al. Small cell lung cancer clinical practice guidelines in oncology. J Natl Compr Canc Netw 2006;4:602–22.
4. Chute JP, Chen T, Feigal E, Simon R, Johnson BE. Twenty years of phase III trials for patients with extensive-stage small-cell lung cancer: perceptible progress. J Clin Oncol 1999;17:1794–801.
5. Cory S, Adams JM. Killing cancer cells by flipping the Bcl-2/Bax switch. Cancer Cell 2005;8:5–6.
6. Jiang SX, Sato Y, Kuwao S, Kameya T. Expression of bcl-2 oncogene protein is prevalent in small cell lung carcinoma. J Pathol 1995;177:135–8.
7. Kaiser U, Schilli M, Haag U, et al. Expression of bcl-2-protein in small cell lung cancer. Lung Cancer 1996;15:31–40.
8. Ikegaki N, Katsumata M, Minna J, Tsujimoto Y. Expression of bcl-2 in small cell lung carcinoma cells. Cancer Res 1994;54:6–8.
9. Ohmori T, Podack ER, Nishio K, et al. Apoptosis of lung cancer cells caused by some anti-cancer agents (MMC, CPT-11, ADM) is inhibited by bcl-2. Biochem Biophys Res Commun 1993;192:30–6.
10. Rudin CM, Kozloff M, Hoffman PC, et al. Phase I study of G3139, a bcl-2 antisense oligonucleotide, combined with carboplatin and etoposide in patients with small-cell lung cancer. J Clin Oncol 2004;22:1110–7.
11. Rudin CM, Salgia R, Wang XF, Green MR, Vokes EE. CALGB 30103: a randomized phase II study of carboplatin and etoposide (CE) with or without G3139 in patients with extensive stage small cell lung cancer (ES-SCLC). J Clin Oncol; 2005 ASCO Annual Meeting Proceedings 2005;23:7168.
12. Oltersdorf T, Elmore SW, Shoemaker AR, et al. An inhibitor of Bcl-2 family proteins induces regression of solid tumours. Nature 2005;435:677–81.

13. Konopleva M, Contractor R, Tsao T, et al. Mechanisms of apoptosis sensitivity and resistance to the BH3 mimetic ABT-737 in acute myeloid leukemia. Cancer Cell 2006;10:375–88.
14. Chauhan D, Hideshima T, Mitsiades C, Richardson P, Anderson KC. Proteasome inhibitor therapy in multiple myeloma. Mol Cancer Ther 2005;4:686–92.
15. Trudel S, Stewart AK, Li Z, et al. The Bcl-2 family protein inhibitor, ABT-737, has substantial antimyeloma activity and shows synergistic effect with dexamethasone and melphalan. Clin Cancer Res 2007;13:621–9.
16. Voskoglou-Nomikos T, Pater JL, Seymour L. Clinical predictive value of the *in vitro* cell line, human xenograft, and mouse allograft preclinical cancer models. Clin Cancer Res 2003;9:4227–39.
17. Lee J, Kotliarova S, Kotliarov Y, et al. Tumor stem cells derived from glioblastomas cultured in bFGF and EGF more closely mirror the phenotype and genotype of primary tumors than do serum-cultured cell lines. Cancer Cell 2006;9:391–403.
18. Whiteford CC, Bilke S, Greer BT, et al. Credentialing preclinical pediatric xenograft models using gene expression and tissue microarray analysis. Cancer Res 2007;67:32–40.
19. Ihaka R, Gentleman R. A Language for Data Analysis and Graphics. Journal of Computational and Graphical Statistics 1996;5:299–314.
20. Gentleman RC, Carey VJ, Bates DM, et al. Bioconductor: open software development for computational biology and bioinformatics. Genome Biol 2004;5:R80.
21. Kaufmann O, Georgi T, Dietel M. Utility of 123C3 monoclonal antibody against CD56 (NCAM) for the diagnosis of small cell carcinomas on paraffin sections. Hum Pathol 1997;28:1373–8.
22. Kuroda J, Puthalakath H, Cragg MS, et al. Bim and Bad mediate imatinib-induced killing of Bcr/Abl+ leukemic cells, and resistance due to their loss is overcome by a BH3 mimetic. Proc Natl Acad Sci U S A 2006;103:14907–12.
23. Chauhan D, Velankar M, Brahmandam M, et al. A novel Bcl-2/Bcl-X(L)/Bcl-w inhibitor ABT-737 as therapy in multiple myeloma. Oncogene 2007;26:2374–80.
24. Kline MP, Rajkumar SV, Timm MM, et al. ABT-737, an

inhibitor of Bcl-2 family proteins, is a potent inducer of apoptosis in multiple myeloma cells. Leukemia 2007;21:1549–60.
25. Deng J, Carlson N, Takeyama K, Dal Cin P, Shipp M, Letai A. BH3 profiling identifies three distinct classes of apoptotic blocks to predict response to ABT-737 and conventional chemotherapeutic agents. Cancer Cell 2007;12:171–85.
26. Perez-Soler R, Kemp B, Wu QP, et al. Response and determinants of sensitivity to paclitaxel in human non-small cell lung cancer tumors heterotransplanted in nude mice. Clin Cancer Res 2000;6:4932–8.
27. Bachmann PS, Gorman R, Mackenzie KL, Lutze-Mann L, Lock RB. Dexamethasone resistance in B-cell precursor childhood acute lymphoblastic leukemia occurs downstream of ligand-induced nuclear translocation of the glucocorticoid receptor. Blood 2005;105:2519–26.
28. Zhou HB, Chen JJ, Wang WX, Cai JT, Du Q. Anticancer activity of resveratrol on implanted human primary gastric carcinoma cells in nude mice. World J Gastroenterol 2005;11:280–4.
29. Lin X, Morgan-Lappe S, Huang X, et al. 'Seed' analysis of off-target siRNAs reveals an essential role of Mcl-1 in resistance to the small-molecule Bcl-2/Bcl-XL inhibitor ABT-737. Oncogene 2007;26:3972–9.
30. van Delft MF, Wei AH, Mason KD, et al. The BH3 mimetic ABT-737 targets selective Bcl-2 proteins and efficiently induces apoptosis via Bak/Bax if Mcl-1 is neutralized. Cancer Cell 2006;10:389–99.
31. Tahir SK, Yang X, Anderson MG, et al. Influence of Bcl-2 family members on the cellular response of small-cell lung cancer cell lines to ABT-737. Cancer Res 2007;67:1176–83.
32. Yu C, Bruzek LM, Meng XW, et al. The role of Mcl-1 down-regulation in the proapoptotic activity of the multikinase inhibitor BAY 43-9006. Oncogene 2005;24:6861–9.
33. Yang C, Kaushal V, Shah SV, Kaushal GP. Mcl-1 is downregulated in cisplatin-induced apoptosis, and proteasome inhibitors restore Mcl-1 and promote survival in renal tubular epithelial cells. Am J Physiol Renal Physiol 2007;292:F1710–7.

Therapeutic Efficacy of ABT-737, a Selective Inhibitor of BCL-2, in Small Cell Lung Cancer

Christine L. Hann, Vincent C. Daniel, Elizabeth A. Sugar, et al.

Updated version	Access the most recent version of this article at: http://cancerres.aacrjournals.org/content/68/7/2321
Supplementary Material	Access the most recent supplemental material at: http://cancerres.aacrjournals.org/content/suppl/2008/03/25/68.7.2321.DC1

Cited articles	This article cites 32 articles, 13 of which you can access for free at: http://cancerres.aacrjournals.org/content/68/7/2321.full#ref-list-1
Citing articles	This article has been cited by 35 HighWire-hosted articles. Access the articles at: http://cancerres.aacrjournals.org/content/68/7/2321.full#related-urls

E-mail alerts	Sign up to receive free email-alerts related to this article or journal.
Reprints and Subscriptions	To order reprints of this article or to subscribe to the journal, contact the AACR Publications Department at pubs@aacr.org.
Permissions	To request permission to re-use all or part of this article, use this link http://cancerres.aacrjournals.org/content/68/7/2321. Click on "Request Permissions" which will take you to the Copyright Clearance Center's (CCC) Rightslink site.